Original Article

Metal Artifact Reduction in Dental Computed Tomography Images Based on Sinogram Segmentation Using Curvelet Transform Followed by Hough Transform

Mehran Yazdi, Maryam Mohammadi

Laboratory of Signal and Image Processing, School of Electrical and Computer Engineering, Shiraz University, Shiraz, Iran

Abstract

In X-ray computed tomography (CT), the presence of metal objects in a patient's body produces streak artifacts in the reconstructed images. During the past decades, many different methods were proposed for the reduction or elimination of the streaking artifacts. When scanning a patient, the projection data affected by metal objects (missing projections) appear as regions with high intensities in the sinogram. In spiral fan beam CT, these regions are sinusoid-like curves on sinogram. During the first time, if the metal curves are detected carefully, then, they can be replaced by corresponding unaffected projections using other slices or opposite views; therefore, the CT slices regenerated by the modified sonogram will be imaged with high quality. In this paper, a new method of the segmentation of metal traces in spiral fan–beam CT sinogram is proposed. This method is based on a sinogram curve detection using a curvelet transform followed by 2D Hough transform. The initial enhancement of the sinogram using modified curvelet transform coefficients is performed by suppressing all the coefficients of one band and applying 2D Hough transform to detect more precisely metal curves. To evaluate the performance of the proposed method for the detection of metal curves in a sinogram, precision and recall metrics are calculated. Compared with other methods, the results show that the proposed method is capable of detecting metal curves, with better precision and good recovery.

Keywords: *Curvelet transform, dental CT images, metal artifact reduction, sinogram*

Introduction

For dental computed tomography (CT) scanners, metal implants such as prosthetic devices, dental filling, surgical clips, and electrodes within the field of view of a CT scanner can create severe artifacts in the reconstructed images. Indeed, metals are considered opaque to X-ray beam, because the atomic numbers of the metals are much higher than those of the human tissues and the bones. The nonlinearity caused by the opacity produces corruption on sinogram. When filtered back projection (FBP) is applied to such a sinogram as reconstruction algorithm, the corruption produces black and white streaks named as metal artifacts in tomography images.

Several algorithms and techniques have been developed to reduce metal artifacts, and they are collectively called as metal artifact reduction (MAR) techniques. Most of the MAR techniques consider the metal objects as missing data.[1] These missing data can be (1) recovered from the corrupted original data (iterative reconstruction methods), (2) completely replaced by synthetic data on the sinograms (projection completion/correction methods), or (3) corrected on projection data (reconstruction correction methods).[2]

Most publications on the MAR methods are based on the segmentation of metallic objects in the CT image followed by a forward projection of the metal-only image to produce a synthetic sinogram, an interpolation in sinogram, and a back projection of the modified sinogram to reconstruct a reduced artifact image.[3-5] Many disadvantages are related to these methods such as inaccuracy in detecting metallic objects when the streak artifacts

How to cite this article: Yazdi M, Mohammadi M. Metal Artifact Reduction in Dental Computed Tomography Images Based on Sinogram Segmentation Using Curvelet Transform Followed by Hough Transform. J Med Sign Sens 2017;7:145-52.

Address for correspondence:
Dr. Mehran Yazdi, Laboratory of Signal and Image Processing, School of Electrical and Computer Engineering, Shiraz University, Shiraz, Iran.
E-mail: yazdi@shirazu.ac.ir

Website: www.jmss.mui.ac.ir

are present and inexactness of synthetic sinogram, since the exact parameters of scanner are usually unknown. Although many papers used original CT image segmentation to reduce metal artifacts, most efficient methods for an MAR work on the sinogram. Direct segmentation of metal traces in sinograms makes it efficient and different from current methods that perform segmentation in reconstructed images. Implementing segmentation and correction directly in original sinograms would avoid the need for a computationally complex forward projection (or the disadvantage associated with using artificial raw data). Moreover, such an approach can also correct for metal artifacts that originate from prosthesis, which is positioned out of the field of view.

As a geometrical approach, sinusoid-like curves on sinogram produced by metal objects are extensively studied by Liu *et al.*[6] More elaborately, mechanisms of tomographic projections are used to find layout of metals. The corrupted metallic projections are roughly identified in a sinogram, and this sinogram shall be projected backward to generate a tomogram. Koseki *et al.*[7] discussed a method which replaces potentially corrupted areas with zero, and then the modified gray scale sinogram is backward projected. In this method however, the detected metallic projection areas may be confused with areas having original zero values. In general, the metal-only tomogram is forward projected into a metal-only sinogram, and then the values in the identified metal-corrupted areas can be replaced by various approaches, such as linear interpolation,[8] wavelet interpolation,[9] or simple subtraction.[10]

In our work, a new method of the segmentation of metal traces in spiral fan–beam CT sinogram is proposed. This method is based on a sinogram segmentation using a curvelet transform and 2D Hough transform. Two important features of curvelet transform are anisotropy scaling law and the directionality, which make it capable of better analyzing the images than by other multi-scale transforms. Candes *et al.*[11] introduced the second generation of curvelet transform which is faster and simpler than the first version, and we also used the second generation of curvelet transform, that is, discrete curvelet transform (DCT) to find metal traces in sinogram. The DCT was introduced by Candes *et al.*[11] in two forms, the wrapping version and the unequally spaced FFT (USFFT) version. Since the wrapping version is faster and invertible up to numerical precision, while the USFFT version is only approximately invertible, so we use only the wrapping version throughout this paper.

In the second step, the Hough-transform method based on the equation of the fan–beam sinogram is applied to the output of curvelet transform for determining all the sinusoid-like curves belonging to metal traces. Finally, to make the segmentation method more accurate, a post-processing step is used followed by applying an interpolation technique in the segmented regions.

Related Work

According to our exhaustive search in the literature, a few works tried to segment the original CT sinogram into metal and nonmetal regions to perform MAR algorithms. Actually, most of the MAR methods worked on forward projection of CT images instead of using original sinogram. Two excellent surveys in this field are the works performed by Rinkel *et al.*[12] and Desai and Kulkarni.[13] Here, we elaborate some MAR methods proposed in the first category. Safdari *et al.*[14] proposed to segment a CT image containing metal objects using Fuzzy C means and then using Radon transform to create its sinogram and metal traces. Next, by an interpolation technique, they modified sinogram and reconstructed a metal artifact-reduced CT image using filtered back projection. To overcome the challenges of working on raw data, Abdoli *et al.*[15] used a virtual sinogram space. They first segmented metallic objects in original CT images using a thresholding technique, and then by forward projection, they created a virtual sinogram, in which the bins affected by metallic objects are obtained. Next, they proposed a weighting strategy by keeping different bins in neighborhood of affected bins and using them to substitute missing projections and correct sinogram. They also use genetic algorithm to find optimal weighting coefficients. Finally, the reconstructed images with MAR were obtained using filtered back projection of corrected sinogram. Their results on dental artifacts showed very good performance. In Li *et al.*'s study,[16] Zhang *et al.* compared a different strategy for replacing the missing projections in sinogram produced by the forward projection of CT images and concluded that an inpainting algorithm based on a fractional order total variation produces better quantitative results.

As we mentioned before, although most of the MAR methods worked on CT images, few works used original sinogram for the MAR. One reason can be the unavailability of original sinogram in most cases, and another reason may be the complexity in working on raw data and sinogram of CT scanners.

Here, we elaborate two main works related to what we will do in this paper. Liu *et al.*[6] suggested a method, in which the metallic objects were detected in the original sonogram in two steps. First, since the metallic objects have higher intensities than the surrounding tissue does, a thresholding technique was used. Thereafter, a set of sinusoidal curves are put in the projection data to determine the complete set of the missing projections. In this way, by using the properties of sinusoidal curves of

metallic textures in sinogram, the affected projections are separated from other projection data. The projections can be amended by subtracting a value, which depends on the attenuation coefficient of the metal implant and the maximum intensity in every projection angle.

In another method,[17] first the original sonogram is binarized by a threshold that separates bright sinusoidal curves on sinogram. Then a simple, nonfiltered back projection is applied on the binarized sinogram; therefore, metal can be identified as an area in tomogram, where their value is at the highest. In the next step, by a forward projection of metal-only tomogram, metal-only sinogram is obtained. Therefore, the values that are corrupted by metals in original sinogram can be detected. These values are then replaced by a linear interpolation. Finally, filtered back projection is applied to the modified sinogram to produce a tomogram without metal artifacts.

Proposed Method

In our work, the suppression of the metal artifacts is performed based on the segmentation of the missing projections in the original sinogram. To do that, we use some techniques to find bright and consistent sinusoid-like curves on sinogram. The proposed method consists of following steps.

Step 1: Contrast sinogram enhancement

As the values of adjacent projections are so close to each other, a contrast enhancement on sonogram can improve the task of segmentation. First, unsharp filtering[18] is used for contrast sonogram enhancement. Next, the curvelet transform[19] is used to analyze edges and enhance the sinogram contrast. The curvelet transform is a new multiscale approach to represent edges.[20] Consequently, our proposed method can efficiently segment metal traces in spiral fan–beam CT sinogram using curvelet transform. This can be obtained by modifying the curvelet coefficients. First, we apply a fast DCT on sinogram by using wrapping method.

As illustrated in Eq. (1), the output will be a collection of coefficients $C(j,l,k)$ indexed by a scale $''j''$, an orientation $''l''$, and spatial position parameter $''k''$.

$$C(j,l,k) = \sum_{j,k,l} f, \phi_{j,l,k}\phi_{j,l,k} \quad (1)$$

where $\phi_{j,l,k}$ is the family of curvelet functions.

The scale levels are divided into three levels, namely coarse level, detail level, and fine level. The low-frequency coefficients contain general information about the original image and are also corresponding to information present in coarse level. High-frequency coefficients are distributed into fine and detail levels. The edge information is available only in the increasing scale of fine levels.

To modify the coefficients of curvelet, the minimum value of coarse level is obtained, and then all the coefficients of this level are replaced by this value. Finally, the inverse curvelet transform of the enhanced sinogram is computed.[20] The result of this step can be seen in Figure 1a.

Step 2: Filtering

Here, Gaussian filter is used to remove unwanted regions of the sinogram. To do that, we subtract the original sinogram from Gaussian filtered sonogram, and we obtain an enhanced version of sonogram. Figure 1b shows the result of this step.

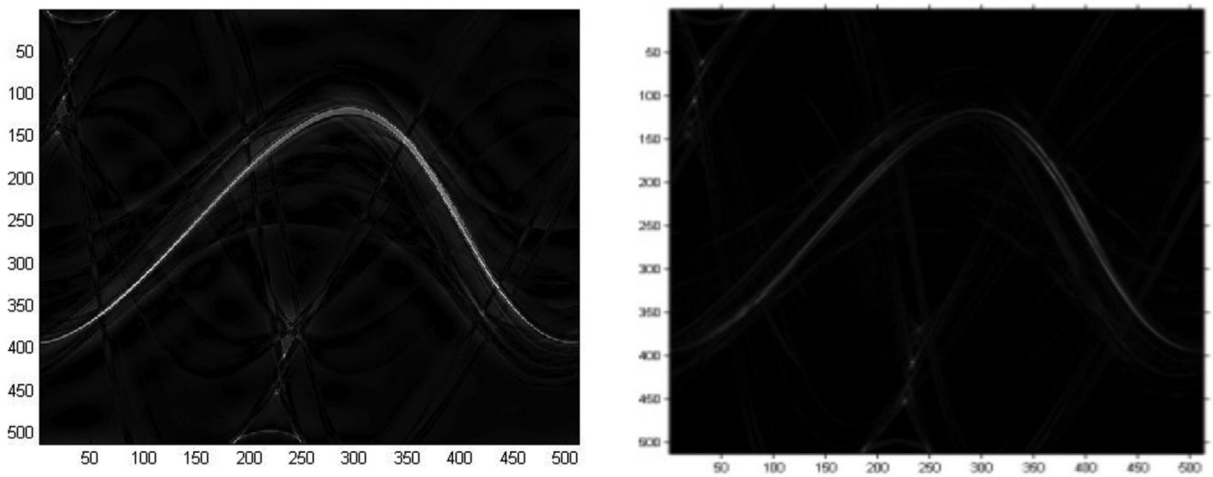

Figure 1: (a) Contrast sinogram enhancement by modifying the coefficients of curvelet. (b) Removing unwanted regions of sinogram

Then, an appropriate threshold that separates opaque areas from others is used; hereby, a black and white sinogram is produced by binarization. The threshold is obtained empirically and fixed for all sinograms used for segmentation.

Step 3: Applying Hough-transform

Our purpose is to find all of the S-like curves belonging to the metal objects in the sinogram. Hough transform (HT)[18] can detect lines, circles, and other structures if their parametric equation is known, so we can use efficiently HT due to the well-known equations of a fan beam scanner.

The equation of sinogram curves or S-like curves can be derived based on the Figure 2.[21] Assume that a point of the object x is given by its polar coordinates (i.e., r_x and β_x), so the circular trajectory of the X-ray source S that rotates around the object is given by Eq. (2):

$$S = (R\cos(\beta), R\sin(\beta)) \tag{2}$$

where R and β are the respective radiuses of the source trajectory and projection angle. Using the fan–beam geometry in Figure 2, a polar coordinate equation that defines the variable fan angle γ can be derived and used for defining the sinogram equation. This polar coordinate equation is given by:

$$\begin{aligned} tg(\gamma) &= \frac{PA}{PS} \\ PA &= OA\sin(\beta-\beta_x) = r_x\sin(\beta-\beta_x) = r_x\cos(\beta-\beta_x) \\ \rightarrow PS &= R - r_x\cos(\beta-\beta_x)\gamma \\ &= \text{arc } tg\frac{r_x\sin(\beta-\beta_x)}{R-r_x\cos(\beta-\beta_x)} \end{aligned} \tag{3}$$

Details of all the geometric parameters can be found in Figure 2. Eq. (3) can be used to define a sinogram curve $S(r_x,\beta_x)$ as follows:

$$S(r_x,\beta_x) = \left\{(\beta,\gamma)|0\leq\beta\leq2\pi, \gamma = \text{arc } tg\frac{r_x\sin(\beta-\beta_x)}{R-r_x\cos(\beta-\beta_x)}\right\} \tag{4}$$

where r_x can be found from Eq. (5)

$$r_x = \frac{Rtg(\gamma)}{\sin(\beta-\beta_x)+tg(\gamma)\cos(\beta-\beta_x)} \tag{5}$$

Indeed, for each r_x and β_x, there is a sinogram curve or S-like curve. Since any object can be approximated by a collection of points located in parametric space, it is expected its projection to be a set of overlapped S-like curves in the fan–beam sinogram space. For this space, the unknown parameters are r_x and β_x. So we can form a 2D Hough-transform using this parametric space to find the best values for unknown parameters. In the implementation of this Hough-transform, the data detected by the previous step are used. Thus, we have n pixels that may partially describe the boundary of metal region in sinogram. The algorithm of HT is a "voting" algorithm, which is used in parameter space of (r_x,β_x), where we construct a 2D accumulator array for the parameter space (r_x,β_x). The ranges of r_x and β_x are set to $0\leq r_x\leq r_{x,\max}$ and $0\leq\beta_x\leq2\pi$, where $r_{x,\max}$ is determined based on the range of the field of view of scanner device in the practice.

Figure 3 shows the block diagram of the steps of HT algorithm for S-like curve detection in the sinogram.

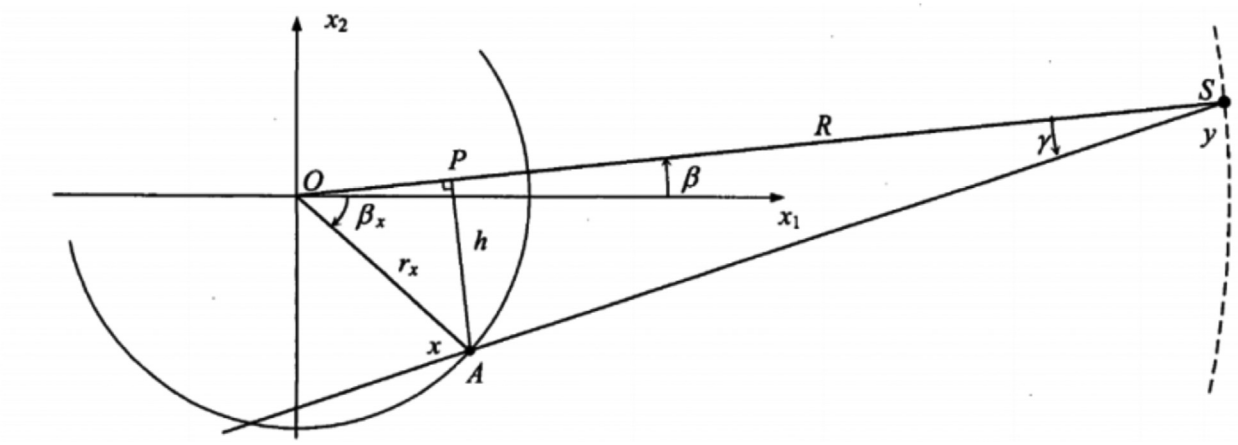

Figure 2: Fan–beam geometry of a fan beam scanner[19]

Finally, each maximum corresponding to r_x and β_x in parametric space represents an S-like curve. Figure 4 shows the results of this step.

Step 4: Post-processing

Although using the mentioned steps can efficiently detect the metallic traces in sinogram, some traces may be missing which will cause inaccuracy in the boundary of detected project region belonging to metal objects. Therefore, we use a postprocessing step to more accurately detect this boundary. To do that, we verify each column of the sinogram corresponding to sampling angles if the detected boundary points are on the ascending or descending part of intensity profile of that column. Figure 5 shows an example of the intensity profile of a column of the sinogram, which contains metal traces. The result of verification indicates that (a) all boundary points are on the ascending or descending part, so these points are

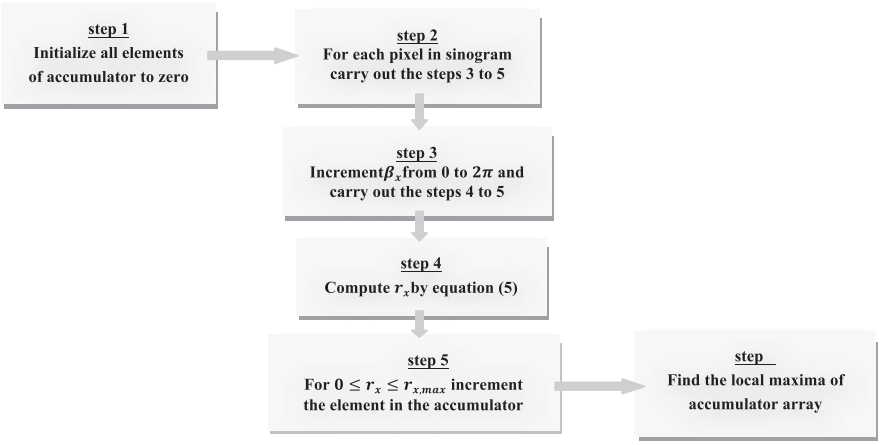

Figure 3: Block diagram of applying Hough-transform algorithm for S-like curve detection

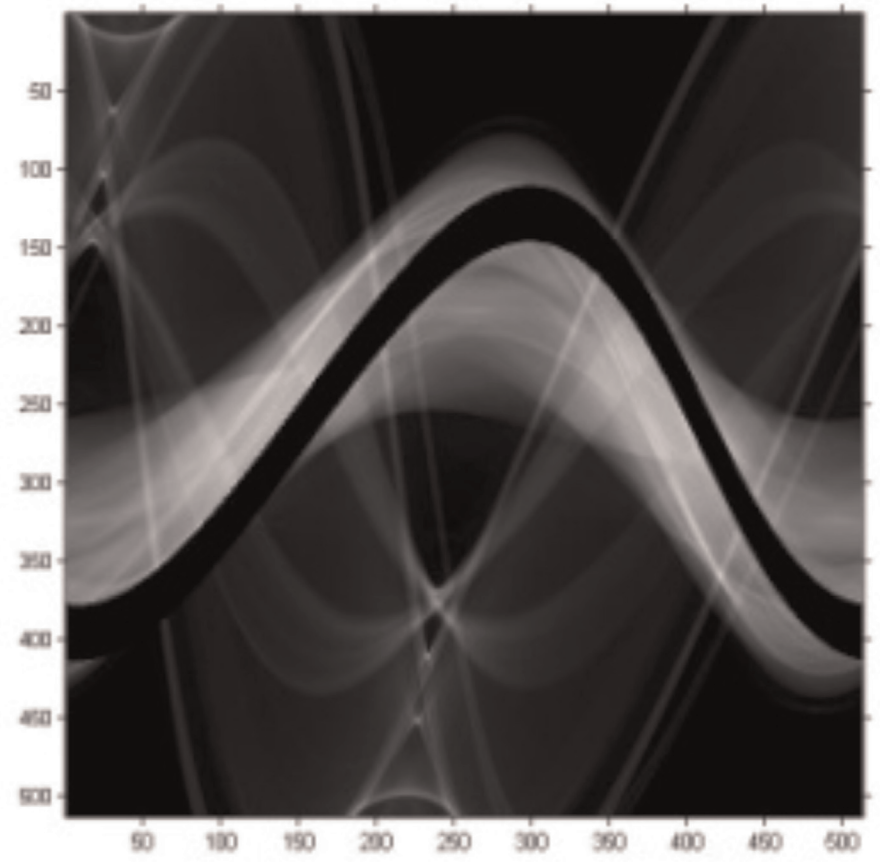

Figure 4: Result of applying Hough-transform algorithm for S-like curve detection

correct and they do not need to be corrected, (b) for each point which is not on the ascending or descending part, we displace it to the nearest point on the ascending or descending part.

Step 5: Image reconstruction

In this step, the original sinogram is enhanced by linear interpolation across the metal traces obtained from previous steps and then a corrected image is regenerated by applying the filtered back projection algorithm. The interpolation method used in our work is the same proposed by Kalender *et al.*[22] The whole process of our proposed MAR method is summarized in Figure 6.

Experimental Results

The scanner was a Siemens Somatom Emotion used in helical mode at 130 kVp (140 mA s) with a pitch of 2. The reconstructed image thickness was 2 mm. In this work, we have tested the proposed method on six patient cases with dental fillings. Although we bring here the results of three patients, for other patients, the same results were obtained. To evaluate the performance of the proposed method in the detection of metal traces in sinogram, precision and recall metrics have been used based on the number of pixels that are true positive (P_{TP}), false positive (P_{FP}), and false negative (P_{FN}) as follows.

$$\text{Precision} = \frac{P_{TP}}{P_{TP} + P_{FP}} \quad (6)$$

$$\text{Recall} = \frac{P_{TP}}{P_{TP} + P_{FN}} \quad (7)$$

Figure 7 shows the obtained results by applying our algorithm compared with the method proposed by Liu *et al.*[6] to segment an original sinogram containing

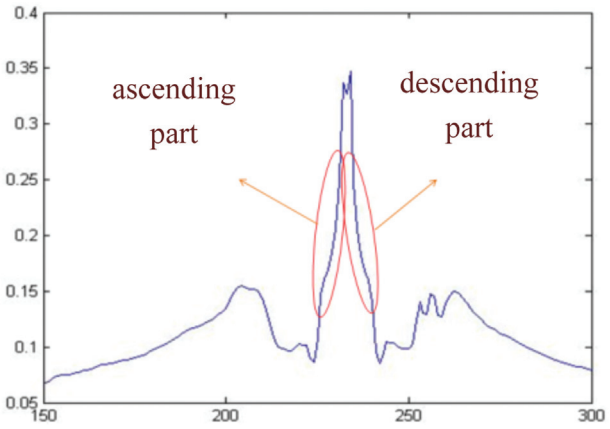

Figure 5: Intensity profile corresponding to a column in the sinogram

Table 1: The results of the quantitative analysis of Figure 7

Comparison parameters	Segmentation of sinogram using "Sinusoidal Amendment"[6]	Segmentation of sinogram using the proposed method
P_{TP}	59,615	145,168
P_{FP}	1514	12
P_{FN}	102,011	16,458
Precision	0.9752	0.9999
Recall	0.3688	0.8982

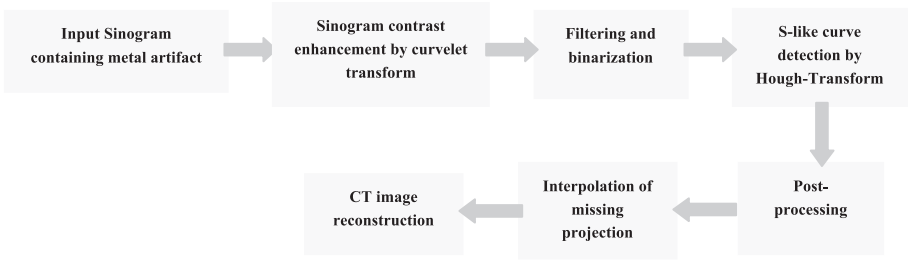

Figure 6: Schematic diagram of the proposed MAR method

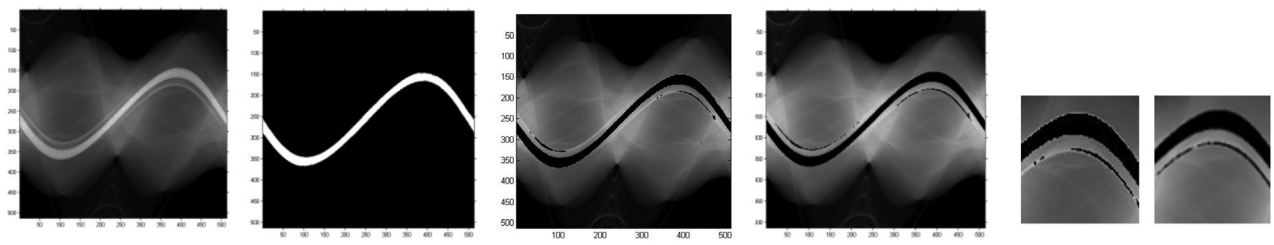

Figure 7: (a) Original sinogram. (b) Metal traces obtained manually in original sinogram. (c) Segmentation of metal traces in sinogram by applying the method of reference.[6] (d) Result of the proposed method. (e) A zoomed region in (c). (f) A zoomed region in (d)

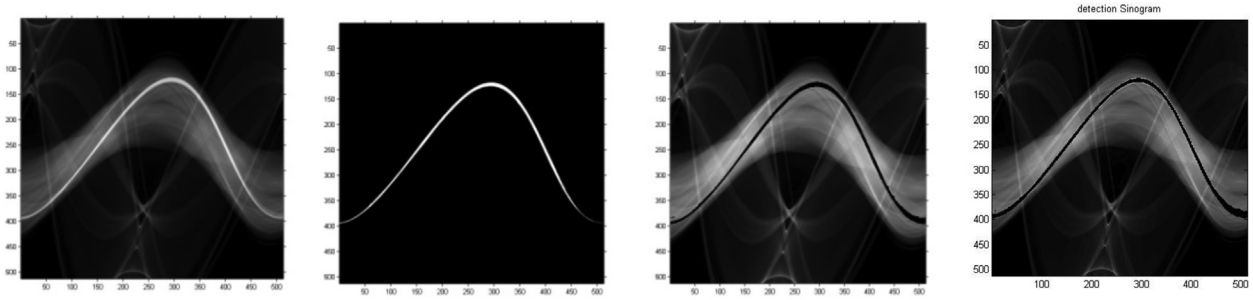

Figure 8: (a) Original sinogram. (b) Metal traces obtained manually in original sinogram. (c) Segmentation of metal traces in sinogram by applying the method of reference.[6] (d) Result of the proposed method

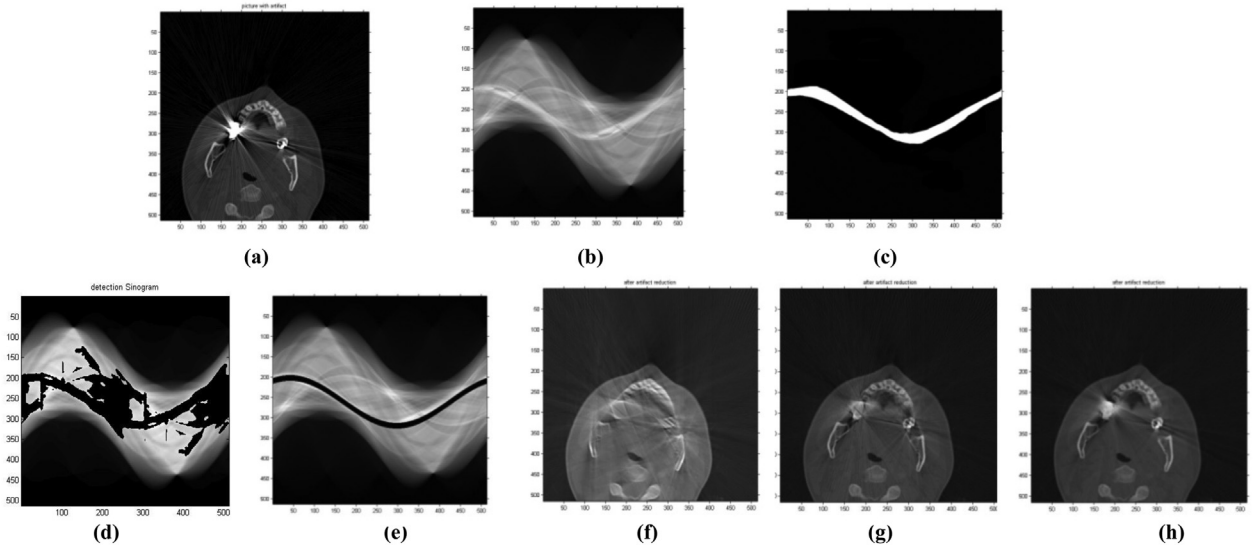

Figure 9: (a) Original CT image. (b) Original sinogram. (c) Metal traces obtained manually in original sinogram. (d) Segmentation of metal traces in sinogram by applying the method of reference.[6] (e) The result of segmentation using the proposed method. (f) Reconstructed image after the interpolation of sinogram shown in (d). (g) The result of method proposed by reference.[14] (h) Reconstructed image after the interpolation of sinogram shown in (e)

Table 2: The results of the quantitative analysis of Figure 8

Comparison parameters	Segmentation of sinogram using "Sinusoidal Amendment"[6]	Segmentation of sinogram using the proposed method
P_{TP}	83,646	152,634
P_{FP}	2396	30
P_{FN}	82,824	13,836
Precision	0.9722	0.9998
Recall	0.5025	0.9169

Table 3: The results of the quantitative analysis of Figure 9

Comparison parameters	Segmentation of sinogram using "Sinusoidal Amendment"[6]	Segmentation of sinogram using the proposed method
P_{TP}	29,157	48,412
P_{FP}	65,759	105,053
P_{FN}	22,712	3457
Precision	0.3072	0.3155
Recall	0.5621	0.9334

metal traces scanned from dental part of the body. For better comparing the results, Figure 7e and f shows a same zoomed region in segmented sonogram of both methods. As can be seen, in our method, the metal traces are well detected compared to that of other methods. Table 1 also shows the recall and precision for segmented regions of Figure 7. As can be seen, the proposed algorithm achieved a much better performance.

A more complex case is when the metal object is very small. Figure 8 and corresponding quantitative comparisons in Table 2 also confirm a better performance of the proposed algorithm. Finally, we tested the performance of algorithms on reconstructed CT images after applying the modifications on sinogram. For this experiment, Figure 9 and Table 3 show the visual and quantitative comparisons, respectively. Here, the performance of the proposed algorithm is much superior to other methods. By

comparing visually the results of Figure 9g and h, we can also see that our method performs better in reducing artifact than the method proposed by Safdari *et al.*,[14] which is based on CT image segmentation. We have also asked a radiologist to evaluate the results, and based on his opinion, our results are very promising in CT MAR.

Conclusion

The method presented in this paper is a MAR algorithm for dental CT scanners based on modifying the original sinogram before using it for reconstruction process to generate CT images. To segment the sinogram into metal and nonmetal traces, at first the DCT was used to better extract the edges between metal traces and nonmetal traces in the sinogram. Next, we applied Hough-transform to accurately detect sinusoid-like curves belonging to metal traces. In the final step, a postprocessing algorithm was used to correct false detection in the previous steps. The experimental results demonstrate the superior performance of the proposed algorithm compared to other related methods.

Financial support and sponsorship

Nil.

Conflicts of interest

There are no conflicts of interest.

References

1. Man BD, Nuyts J, Dupont P. Reduction of metal streak artifacts in X-ray computed tomography using a transmission maximum a posteriori algorithm. IEEE Trans Nucl Sci 2000;47:977-81.
2. Tohnak S, Mehnert A, Mahoney M, Crozier S. Dental CT metal artefact reduction based on sequential substitution. Dentomaxillofacial. Radiology 2011;40:184-90.
3. Abdoli M, Ay MR, Ahmadian A, Zaidi H. A virtual sinogram method to reduce dental metallic implant artefacts in computed tomography-based attenuation correction for PET. Nucl Med Commun 2010;31:22-31.
4. Kim Y, Yoon S, Yi J. Effective sinogram-inpainting for metal artifacts reduction in X-ray CT images. IEEE Int Conf Image Process 2010;597-600.
5. Yazdi M, Beaulieu L. A novel approach for reducing metal artifacts due to metallic dental implants. IEEE Nucl Sci Symp Conf Rec 2006;4:2260-3.
6. Liu JJ, Watt-Smith SR, Smith SM. CT reconstruction using FBP with sinusoidal amendment for metal artifact reduction. Proc. VIIth Digital Image Computing; 2003. p. 10-2.
7. Koseki M, Hashimoto S, Sato S, Kimura H, Inou N. CT image reconstruction algorithm to reduce metal artifact. J Solid Mech Mater Eng 2008;2:374-83.
8. Bracewell RN, Riddle AC. Inversion of fan beam scans in radio astronomy. Astrophys J 1967;150:427-34.
9. Zhao S, Robertson DD, Wang G, Whiting B, Bae KT. X-ray CT metal artifact reduction using wavelets: An application for imaging total hip prostheses. IEEE Trans Med Imaging 2000;19:1238-47.
10. Takahashi Y, Mori S, Kozuka T, Gomi K, Nose T, Tahara T, *et al.* Preliminary study of correction of original metal artifacts due to I-125 seed in postimplant dosimetry for prostate permanent implant brachytherapy. Radiat Med 2006;24:133-8.
11. Candes E, Demanet L, Donoho D, Ying L. Fast discrete curvelet transforms. Multiscale Model Simul 2006;5:861-99.
12. Rinkel J, Dillon WP, Funk T, Gould R, Prevrhal S. Computed tomographic metal artifact reduction for the detection and quantitation of small features near large metallic implants: A comparison of published methods. J Comput Assist Tomogr 2008;32:621-9.
13. Desai SD, Kulkarni L. Comprehensive survey on metal artifact reduction methods in computed tomography images. In: Medical Imaging: Concepts, Methodologies, Tools, and Applications. USA: IGI Global; 2017. p. 1281-302.
14. Safdari M, Karimian A, Yazdchi MR. A new method for metal artifact reduction in CT scan images. Iran J Med Phys 2013;10:139-46.
15. Abdoli M, Ay MR, Ahmadian A, Dierckx RA, Zaidi H. Reduction of dental filling metallic artifacts in CT-based attenuation correction of pet data using weighted virtual sinograms optimized by a genetic algorithm. Med Phys 2010;12:6166-77.
16. Li Y, Chen Y, Hu Y, Oukili A, Luo L, Chen W, *et al.* Strategy of computed tomography sonogram inpainting based on sinusoid-like curve decomposition and eigenvector-guided interpolation. J Opt Soc Am A Opt Image Sci Vis 2012;29:153-63.
17. Kobayashi K, Katsumata A, Ito K, Aoki T. A practical metal artifact reduction method for dental cone beam CT scanners. 19th International Conference in Pattern Recognition. 2008; p. 408-11.
18. Starck JL, Candès EJ, Donoho DL. The curvelet transform for image denoising. IEEE Trans Image Process 2002;11: 670-84.
19. Gonzalez RC, Woods RE. Digital Image Processing. 3rd edition. USA: Prentice-Hall; 2007.
20. Kalaivani M, Jeyalakshmi MS, Aparna V. Extraction of retinal blood vessels using curvelet transform and Kirsch's templates. Int J Emerg Technol Adv Eng 2012;2:360-3.
21. Zamyatin AA, Nakanishi S. Sinogram correction methods using sinogram decomposition. IEEE Nucl Sci Symp Conf Rec 2006;6:3438-40.
22. Kalender WA, Hebel R, Ebersberger J. Reduction of CT artifacts caused by metal implants. Radiology 1987;164:576-7.